



HHS Public Access

Author manuscript

Hepatology. Author manuscript; available in PMC 2021 May 01.

Published in final edited form as:

Hepatology. 2021 May ; 73(5): 1855–1867. doi:10.1002/hep.31504.

Unique cholangiocyte-targeted IgM autoantibodies correlate with poor outcome in biliary atresia

Yuhuan Luo, MD,

University of Colorado School of Medicine

Dania Brigham, MD,

Children's Hospital Colorado

Joseph Bednarek,

University of Colorado School of Medicine and University of Utah

Richard Torres,

University of Colorado School of Medicine

Dong Wang, PhD,

University of Colorado School of Medicine

Sara Ahmad,

University of Colorado School of Medicine

Cara L. Mack, MD,

University of Colorado School of Medicine, Children's Hospital Colorado

In conjunction with the Childhood Liver Disease Research Network

Abstract

Background & Aims: The etiology of biliary atresia (BA) is not known and is likely multifactorial, including a genetic predisposition, a viral or environmental trigger, an aberrant autoimmune response targeting cholangiocytes and unique susceptibilities of the neonatal bile ducts to injury. Damaged cholangiocytes may express neo self-antigens and elicit autoreactive T cell-mediated inflammation and B cell production of autoantibodies. The aim of this study was to discover novel autoantibodies in BA that correlated with outcomes.

Approach & Results: An autoantigen microarray encompassing ~9,500 autoantigens was utilized to screen for serum IgM and IgG autoantibodies in BA patients or other liver disease controls. Validation of candidate autoantibodies by ELISA on a second cohort of subjects (6–12 months post-Kasai portoenterostomy), and correlations of autoantibodies with outcomes were performed (serum bilirubin levels and need for liver transplant in first 2 years of life). Mean anti-

Contact Information. Cara L. Mack, MD, Hewitt/ Andrews Chair in Pediatric Liver Disease, Professor of Pediatrics, Section of Pediatric Gastroenterology, Hepatology & Nutrition and the Digestive Health Institute, University of Colorado School of Medicine, Children's Hospital Colorado, Box B290, 13123 E. 16th Ave, Aurora, CO 80045, phone: 720-777-6470; FAX: 720-777-7277, cara.mack@childrenscolorado.org.

This article has been accepted for publication and undergone full peer review but has not been through the copyediting, typesetting, pagination and proofreading process, which may lead to differences between this version and the [Version of Record](#). Please cite this article as doi: [10.1002/HEP.31504](https://doi.org/10.1002/HEP.31504)

chitinase 3-like 1 (CHI3L1), anti-delta-like ligand (DLL-4) and anti-surfactant protein D (SFTPD) IgM autoantibodies in BA were significantly higher compared to controls and IgM autoantibody levels positively correlated with worse outcomes. Immunofluorescence revealed cholangiocyte-predominant expression of CHI3L1, DLL-4 and SFTPD. The humoral autoantibody response was associated with C3d complement activation and T cell autoimmunity, based on detection of cholangiocyte-predominant C3d co-staining and peripheral blood autoreactive T cells specific to CHI3L1, DLL-4 and SFTPD, respectively.

Conclusions: Biliary atresia is associated with cholangiocyte-predominant IgM autoantibodies in the first year after Kasai portoenterostomy. Anti-CHI3L1, anti-DLL-4 and anti-SFTPD IgM autoantibody correlations with worse outcomes and the detection of C3d on cholangiocytes and antigen-specific autoreactive T cells suggests that autoimmunity plays a role in the ongoing bile duct injury and progression of disease.

Keywords

Cholangiocyte; Cholestasis; Complement activation; Humoral autoimmunity

Biliary atresia (BA) is the most frequent cause of neonatal cholestasis and the most frequent indication for pediatric liver transplant, accounting for ~50% of all transplants in children(1). The etiology of BA is not known and is likely multifactorial, including a genetic predisposition, a viral or environmental trigger, an aberrant autoimmune response targeting cholangiocytes and unique susceptibilities of the neonatal bile ducts to injury(2). Damaged cholangiocytes may express “neo self-antigens” and elicit autoreactive T cell-mediated inflammation and B cell production of autoantibodies. Previous research has demonstrated the importance of T cell responses in bile duct injury in BA and the rotavirus-induced mouse model of BA(3). However, evidence for the role of B cells in BA pathogenesis is limited. In the mouse model of BA, rotavirus-infected mice deficient in Ig- α (a component of the B cell receptor necessary for antibody production and antigen presentation), did not develop BA(4, 5), suggesting a crucial role for B cells in disease pathogenesis. Evidence for B cell activation in human BA includes the finding of increased intrahepatic periductal B cell infiltrates at the time of diagnosis and at transplant(5). Analysis of hilar lymph nodes contiguous with the most proximal biliary remnants in BA patients revealed that 51% of BA infants (versus 0% of controls) had one or more well-formed, reactive germinal centers, suggesting antigen-driven B cell activation(6). The specificity of the antigen(s) and why only half of the BA patients had mature germinal centers is not well understood.

IgM antibody levels rise rapidly during the first months of life, attaining 75% of adult levels by 1 year of age(7, 8), while neonatal production of IgG does not reach peak levels until 5 years of age. Neonates have robust IgM responses and have been shown to generate “natural autoantibodies” to a select set of self-antigens at birth(9). In that study the authors concluded that based on the presence of some major disease-associated self-antigens within the IgM repertoire, pathologic autoimmune disease could arise through a lapse in the regulation of otherwise benign, “natural” autoimmunity.

Detection of autoantibodies in human BA has been limited to either the identification of autoantibodies that were previously discovered in the mouse model of BA (i.e. alpha-enolase

antibodies)(10) or autoantibodies previously discovered in other autoimmune biliary diseases (i.e. primary biliary cholangitis-specific autoantibodies)(11). The aim of the current study was to discover novel IgM and/ or IgG autoantibodies in human BA utilizing an autoantigen microarray encompassing ~9,500 autoantigens. Validation of candidate autoantibodies discovered from the microarray was performed on an additional cohort of patients. A sub-aim of the study was to determine if the autoantibodies correlated with outcomes (serum bilirubin levels and need for liver transplant), suggesting a role for these autoantibodies in disease pathogenesis.

Materials and Methods.

Patient serum samples.

Serum samples, demographics and outcomes data were obtained through the Childhood Liver Disease Research Network (ChiLDReN), which entails 13 sites in the United States and Canada and is funded by the NIDDK ([clinicaltrials.gov NCT01854827](https://clinicaltrials.gov/NCT01854827)). Ethical approval was obtained at each site and at the Data Coordinating Center; parents or legal guardians of the participants provided written informed consent. Serum samples analyzed included an exploratory cohort: BA N=10, other liver disease controls N=10; age range 1–5 years: IgG and IgM analyses; Supplementary Table 1) and a validation cohort (BA N=57; other liver disease controls N=58; age range 6–12 months post-Kasai: IgM analysis; Table 1).

Microarray.

The Invitrogen ProtoArray Human Protein Microarray v5.0 (9,480 human proteins) assay and statistical analyses were performed by UT Southwestern Genomics and Microarray Core Facility. In short, protein microarrays were blocked with phosphate-buffered saline (PBS) containing 1% bovine serum albumin (BSA) and 0.1% Tween-20 before incubation with serum (1:500) and Cy3-conjugated anti-human IgM and Alexa Fluor 647-conjugated anti-human IgG. The arrays were scanned using an Axon Genepix 400B fluorescent microarray scanner. Genepix 6.0 software was used to align the scanned image to the template and to determine the pixel intensities for each spot on the array. The reported pixel intensity was calculated as the average of duplicate signals after background subtraction. The software tool used was the Prospector software (Invitrogen), which is based on M-statistics. This software performs background subtraction, normalization of the signals, and analysis of the differences between the two groups of patients. When comparing two groups, a cutoff for positivity is calculated for each protein using M-statistics. The proportion of subjects with an immune response above the cutoff value is counted and a P-value representing the significance of the difference between both groups is calculated.

ELISA.

96-well microplates were coated with 5 µg/ml of recombinant human proteins Chitinase 3-like 1 (CHI3L1), delta-like ligand 4 (DLL-4) (Sino Biological) or surfactant protein D (SFTPD) (R&D Systems), washed with PBS/0.1 % Tween[®]20, blocked with PBS/ 1% BSA and incubated with 1:100 diluted human sera or negative control (BSA only), followed by HRP-conjugated anti human IgM (1:5000) and tetramethylbenzidine substrate (Thermo

Scientific, USA). The reaction was stopped with H₂SO₄ and the optical density (OD) was determined at 450nm using an automated spectrophotometer (BioTek). A standard curve was generated for each autoantibody utilizing commercially available antibodies and expressed as relative units (RU)/ml. Serum sample concentrations were calculated from the standard curves. Background OD levels based on BSA controls were subtracted from each experimental sample read.

Cell Culture and immunofluorescence.—The H69 cell line is an SV40-transformed intrahepatic normal bile duct epithelial cell line provided by N. Larusso laboratory (Mayo Clinic, Rochester, MN). The HepG2 cell line is a hepatocellular carcinoma cell line provided by F. Suchy laboratory (UC Denver Anschutz, CO, USA). Human liver tissues were obtained from Children’s Hospital Colorado (IRB #12–0069). The cells or human liver sections were fixed in 4% paraformaldehyde, incubated with 0.2% Triton X-100/PBS, blocked with 3% BSA/PBS, incubated with monoclonal antibodies anti-human CHI3L1, DLL4, SFTPD, C3d, CD3, desmin or cytokeratin 7 at 1:100 dilutions, and followed by incubation with Alexa Flour 555- or 488-conjugated secondary antibodies and mounting media containing DAPI (Vector Labs, USA). Tissue and cells were visualized using the Zeiss LSM 710 microscope. The areas containing CK7⁺ cells (cholangiocytes) were identified using ImageJ software (ImageJ, NIH) and quantitative fluorescence intensity analysis of the amount of autoantigen expression per μm^2 of CK7⁺ cells was calculated. Three to five CK7⁺ cellular regions were analyzed per sample. Average mean gray value of each autoantigen was determined.

FluoroSpot.

Human IFN γ /IL2, IL17A FluoroSpot kits (MabTech, USA): Previously frozen Ficoll-gradient purified peripheral blood mononuclear cells (IRB #12–0069) were incubated in culture (25×10^5 cells/well) with 1 $\mu\text{g}/\text{ml}$ of either human CHI3L1 (Sino Biological), DLL4 (Sino Biological) or SFTPD protein (R&D) to FluoroSpot wells that were previously coated with cytokine capture antibodies. Cytokine detection fluorophore-conjugated antibodies were added and FluoroSpot analysis was performed with an automated FluoroSpot reader (ImmunoSPOT S6 ULTIMATE Analyzer). Positive control wells contained PHA and negative control wells contained media only.

Statistical analyses.

Values are expressed as mean \pm standard deviation. For continuous variables, the Student *t* test was used for comparison between two groups. Chi squared test, two-sided, was performed to compare differences in frequencies between groups. Correlations were evaluated by the Spearman’s correlation coefficient. Generation of receiver operator curves (ROC) and associated multiple logistic regression analyses were performed with PRISM GraphPad software. Power analysis: The size calculation for the ELISA validation studies was based on the average percent of patients positive for one of the 3 candidate autoantibodies in BA versus controls (based on the microarray data). A sample size of 47 per group was required to ensure 80% power at 5% significance to detect a difference between groups. PRISM GraphPad software (La Jolla, CA) was employed for all statistical analyses. P values < 0.05 were considered statistically significant.

Results.

Autoantigen microarray identifies IgM autoantibodies in BA.

IgM and IgG autoantibodies were screened for using an autoantigen microarray that contains 9,480 human proteins (ProtoArray[®]), many of which have been implicated as targets in a variety of autoimmune diseases(12). The exploratory cohort included subjects that had their native liver at the time of serum collection. The age range of 1– 5 years was chosen for this exploratory cohort in order to test both IgM and IgG autoantibody responses in the child (i.e. < 1 years of age the IgG would be predominantly maternal in origin). There were 10 BA patients (age: 32.6±11.3 mons.; 60% female; 60% Caucasian) and 10 controls (Alagille syndrome N=5, A1AT deficiency N=5) (age: 31.4±9.5 mons.; 60% female; 60% Caucasian; Supplementary Table 1). Overall significant differences between groups were identified for 278 autoantigens (results of entire microarray shown in Supplementary Table 2). A significant increase in the mean value of autoantibodies in BA versus controls was identified for 12 IgM autoantibodies and 24 IgG autoantibodies (Figure 1A, Supplementary Figure 1). An autoantibody that warranted further investigation with a validation cohort, termed “candidate autoantibody”, was defined based on a significant increase in the mean value in BA versus controls ($P < 0.05$) and at least 50% of BA subjects with an autoantibody level > 1 standard deviation above the mean of the controls. We were most interested in candidate autoantigens expressed in the liver and/or biliary tree, and searched both the Human Protein Atlas (proteinatlas.org) and Pubmed literature to confirm organ location of protein expression.

Eleven IgM autoantibodies were identified as candidate autoantibodies in BA. Six of the 11 IgM autoantibodies targeted proteins associated with the immune system [CD16b, GM-CSFR, TNRSF4, IL18RAP, G-CSFR, CNTN3 (Ig superfamily)]. This phenomenon of autoantibodies against immune cell proteins has been previously described in the setting of chronic inflammation and infection(13). Due to the non-disease specific nature of the immune-targeted autoantibodies, validation studies of these candidate autoantibodies were not performed. Further analysis of IgM candidate autoantibodies in the validation cohort was considered for the following 5 autoantigens: DLL-4 (delta-like ligand 4), CHI3L1 (chitinase 3-like 1; YKL40), SFTPD (surfactant protein D), CA8 (carbonic anhydrase 8) and CA13 (carbonic anhydrase 13). The liver has moderate to high expression of DLL-4 (protein involved in NOTCH signaling)(14), CHI3L1 (protein involved in tissue remodeling)(15), and CA13 (zinc metalloenzyme). SFTPD protein, a protein involved in cellular homeostasis, is abundant in the lung and has recently been shown to be expressed in hepatocytes and cholangiocytes as well(16). CA8 is not expressed in the liver or biliary tree. Therefore, DLL-4, CHI3L1, CA13 and SFTPD constituted the 4 candidate IgM autoantibodies that warranted further investigation (Figure 1B).

Six IgG autoantibodies were identified as candidate autoantibodies in BA. One of these 6 IgG candidates, anti-DLL-4 IgG, was pursued in validation studies. The other 5 IgG candidate autoantibodies in BA were not pursued in this study due to the following reasons: FAM120C & FLJ46266 (no liver/ biliary expression), UPF3A (mRNA nuclear export

protein), TBC1D7 (protein involved in tuberous sclerosis), and LST1 (immune protein) (Supplementary Figure 1B; blue highlight).

Increased serum anti-CHI3L1, anti-DLL-4 and anti-SFTPD IgM autoantibodies in BA correlates with worse outcomes.

Serum ELISA testing of the 4 candidate IgM autoantibodies was performed on a validation cohort of 115 subjects from ChiLDReN (58 other liver disease controls, 57 BA). The other liver disease controls included Alagille syndrome (N=20), alpha-1 anti-trypsin deficiency (N=21), indeterminate cholestasis (N=6), idiopathic neonatal giant cell hepatitis (N=6), and one each of bile duct paucity, choledochal cyst, cystic fibrosis, progressive familial intrahepatic cholestasis and septo-optic dysplasia. The subjects were similar in age at the time of serum collection, however BA subjects had significantly higher frequencies of female gender and non-Caucasian race, as well as higher serum total bilirubin levels (Table 1). Mean anti-CHI3L1, anti-DLL-4 and anti-SFTPD IgM autoantibodies in BA were 2.2 to 3.4-fold higher than those in controls (Figure 2A). There was no difference between groups in anti-CA13 IgM levels and this autoantibody was not pursued in further studies (data not shown). Overall, 53% of BA subjects were positive for at least 1 autoantibody (defined as > 1SD above the mean of the control group). The proportion of BA subjects positive for a specific antibody included 26% for anti-CHI3L1 IgM (control 8.5%; P=0.012), 44% for anti-DLL-4 IgM (control 13.8%; P=0.0003), and 35% for anti-SFTPD IgM (control 10.3%; P=0.0015). In BA, the anti-CHI3L1, anti-DLL-4 and anti-SFTPD IgM autoantibody levels positively correlated with total bilirubin (Figure 2B) and AST (Supplementary Figure 2). In addition, anti-DLL-4 levels positively correlated with APRI score ((Supplementary Figure 2). Anti-CHI3L1, anti-DLL-4 and anti-SFTPD IgM autoantibodies were 1.9 to 2.4-fold higher in BA subjects who received liver transplant in the first 2 years of life compared to those without transplant (Figure 2C). There was no significant difference in the age at the time of Kasai portoenterostomy between those BA subjects without transplant (1.57 ± 0.66 months) or with transplant (2.07 ± 1.23 months) in the first 2 years of life (P=0.08). In addition, we generated receiver operator curves (ROC) for the 3 IgM autoantibodies to determine if the autoantibodies could discriminate BA from controls and to determine how the autoantibodies predicted need for transplant compared to other markers of severity of disease (total bilirubin, APRI). Acceptable AUROC values reflected the ability of anti-DLL4 and anti-CHI3L1 IgM, but not anti-SFTPD, to discriminate BA from controls (Figure 2D). However, the autoantibodies were inferior (AUC 0.64–0.71) to either bilirubin or APRI (AUC 0.87–0.9) at predicting need for liver transplant at 2 years of age (Figure 2E). Multiple logistic regression analyses of the combination of bilirubin and APRI with all three autoantibodies did not increase the predictive value of need for transplant (bilirubin/APRI combined AUC 0.918; bilirubin/APRI/all 3 autoantibodies combined AUC 0.919).

A sub-analysis of the number of IgM autoantibodies that a given BA subject was positive for revealed that 19% were positive for all three IgM autoantibodies, 14% were positive for two autoantibodies, 19% were positive for one autoantibody and 47% were negative for all three IgM autoantibodies (Figure 3). Those BA subjects positive for all three IgM autoantibodies were more likely to be female, had significantly higher total bilirubin and a higher proportion had a liver transplant in the first 2 years of life (three positive IgM

autoantibodies: 82% transplanted; negative for IgM autoantibodies: 37% transplanted) (Table 2).

Validation studies pertaining to the candidate anti-DLL-4 IgG included a separate group of older BA (N=31; age 14.6±2.9 months) and other liver disease controls (N=32; age 14.3±2.6 months) ranging from 12–20 months of age (Supplementary Table 3). The reason for this older validation cohort was due to the fact that in the first year of life the majority of IgG would be maternal in origin. In this cohort there was no significant difference in the mean values of anti-DLL-4 IgG between groups (Supplementary Figure 3).

Cellular immunofluorescence reveals cholangiocyte-predominant expression of CHI3L1, DLL-4 and SFTPD.

It is theorized that the humoral immune response specifically targets cholangiocytes in BA. Therefore, we sought to determine the cellular specificity (hepatocyte versus cholangiocyte) and location (membrane, cytosolic, nuclear) of CHI3L1, DLL-4 and SFTPD proteins. Hepatocytes (HepG2 cell line) and cholangiocytes (H69 cell line) were stained with fluorescent-tagged antibodies to CHI3L1, DLL-4 and SFTPD. Qualitative analysis showed that all 3 proteins are more abundant on cholangiocytes compared to hepatocytes. Cholangiocyte CHI3L1 localized to cytosol, DLL-4 was present predominantly in the cytosol and less so in the nucleus and SFTPD was predominantly nuclear in origin (Figure 4).

Immunofluorescence staining was performed on frozen explant liver tissue from controls (N=10; age: 1.8±0.9 years) and BA (N=10; age: 1.25±0.9 years; P=0.17). Cholangiocytes were identified by cytokeratin 7 (CK7) staining. All 3 autoantigens co-localized predominantly within CK7 positive cells, as compared to hepatocytes. Quantitative fluorescence intensity analysis of the amount of autoantigen expression per μm^2 of CK7 positive cells revealed significant increases in CHI3L1, DLL-4 and SFTPD within cholangiocytes in BA compared to controls (Figure 5).

Autoimmune-associated effector pathways include cholangiocyte-predominant C3d deposition and circulating autoreactive T cells in BA.

In certain disease states, IgM autoantibodies have been shown to activate the complement system and drive pathology(17, 18). One such product of IgM-mediated complement activation is C3d deposition. To determine if cholangiocyte-predominant IgM autoantibodies were triggering complement activation, C3d immunofluorescence was performed on frozen explant liver tissue from controls (N=10; age: 1.8±0.9 years) and BA (N=16; age: 1.07±0.77 years). Marked C3d deposition was identified on cholangiocytes in BA subjects. Quantitative fluorescence intensity analysis of the amount of C3d expression per μm^2 of CK7 positive cells revealed significant increases in C3d that co-localized to cholangiocytes in BA, suggesting a role for IgM-mediated complement activation in bile duct injury (Figure 6A). Comparison of the quantity of C3d deposition between BA subjects who were negative versus positive for all three autoantibodies revealed that subjects who were positive for all three IgM autoantibodies had significantly higher levels of cholangiocyte C3d deposition, suggesting a direct effect of IgM autoantibodies on complement deposition (Figure 6B). In

addition, subjects who were positive for all three autoantibodies had significantly higher amounts of portal tract fibrosis based on quantification of desmin staining (Figure 6B).

In autoimmunity, humoral (B cell) and cellular (T cell) immune responses targeting specific autoantigens often occur in parallel. Antigen-specific autoreactive T cells in organ-specific diseases may circulate in the peripheral blood, reflecting active T cell autoimmune responses(19, 20). Therefore, to provide additional evidence of the significance of the cholangiocyte autoantigens (CHI3L1, DLL-4, SFTPD) in BA autoimmunity, analysis of autoreactive T cells within peripheral blood mononuclear cells (PBMCs) specific to one of the candidate autoantigens was performed. PBMCs from either BA or age-matched other liver disease controls were cultured with CHI3L1, DLL-4, or SFTPD for 48 hours. Antigen-specific T cell activation was measured with ELISPOT, based on T cell production of either IL-2, IFN- γ or IL-17. Significant increases in IL-2 and IFN- γ production in response to either CHI3L1 or SFTPD, and increased IFN- γ production in response to DLL-4 were identified in BA subjects (Figure 6C). There was no significant difference between groups in IL-17 production (data not shown). Furthermore, BA subjects who were positive for all 3 autoantibodies had increased numbers of portal tract CD3⁺ T cells compared to BA subjects who were negative for all autoantibodies (Supplementary Figure 4).

Discussion.

Despite the “wide net” that was cast to search for autoantibodies in BA using a 9,480 autoantigen microarray, the discovery of 3 autoantibodies that are specific to proteins highly expressed in cholangiocytes is quite remarkable. Autoantigen microarrays have been utilized in order to identify novel autoantibodies involved in disease pathogenesis and as diagnostic or prognostic biomarkers(12). This includes novel autoantibody discoveries in inflammatory bowel disease(21) and autoimmune hepatitis(22). In our study, anti-CHI3L1, anti-DLL-4 and anti-SFTPD IgM autoantibodies correlated with poor outcomes (higher bilirubin levels and need for liver transplant) and complement activation, suggesting that the humoral immune response may play a role in disease pathogenesis. In addition, detection of circulating autoreactive T cells specific to CHI3L1, DLL-4 and SFTPD at the time of diagnosis of BA provides further evidence for autoimmunity early in the disease course. Importantly, we have previously shown oligoclonal expansions of both CD4⁺ and CD8⁺ T cells in BA livers, however the specific antigen stimulus leading to this clonality was unknown at the time.(23) Based on the current findings of cholangiocyte-specific autoreactive T cells in the periphery, future studies can now focus on determining if the clonal liver T cell populations are specific to CHI3L1, DLL-4 and/ or SFTPD.

Early studies focusing on autoantibodies in BA identified periductal IgM and IgG deposits along the basement membrane of bile duct epithelia within extrahepatic bile duct remnants in ~40% of BA patients at diagnosis(24). Periductal immunoglobulin deposits and serum autoantibodies, including anti- α -enolase, have been described in the mouse model of BA and in a subset of human infants (IgM) and older children (IgG) with BA(10, 25). Unfortunately α -enolase was not within the Protoarray[®] used in the current study and therefore we were unable to validate this previous finding. A recent study in older BA patients with their native liver involved detection of IgG autoantibodies that are known to be

associated with other autoimmune liver diseases(11). In that study the overall rate of IgG autoantibody positivity in BA was 56.5%, with the majority positive for autoantibodies within a primary biliary cholangitis-specific profile. These previous IgG autoantibody studies in BA were based on known autoantigen targets in either the mouse model of BA or other autoimmune cholangiopathies. The current study is novel in that the search for autoantibodies in BA was unbiased, included both IgM and IgG responses, and explored the majority of autoantigen proteins that are commercially available for analysis.

We discovered 3 novel IgM autoantibodies in infants with BA that target cholangiocyte-associated proteins (CHI3L1, DLL-4 and SFTPD). CHI3L1 (also known as TKL-40) is a glycoprotein that plays a role in angiogenesis, tissue remodeling and fibrogenesis. It is highly expressed in the liver compared to other organs (Illumina Human Body Map 2.0 (<http://genomicdbdemo.bxgenomics.com>)). CHI3L1 expression is increased in the fibrotic liver and CHI3L1 levels in the liver positively correlate with stages of fibrosis, suggesting that this protein is intricately involved in fibrogenesis(15, 26). DLL-4 is a ligand within the Notch pathway and is involved in numerous cell fate/ lineage decisions during embryogenesis and postnatal development, including genesis of the vasculature and biliary tree(27). We have shown that DLL-4 is highly expressed in cholangiocytes and autoantibody responses targeting DLL-4 could inhibit biliary development. Another function of DLL-4 pertains to down regulation of inflammatory molecules such as chemokines(14); inhibition of this anti-inflammatory DLL-4 mechanism in the presence of DLL-4 autoantibodies could contribute to the ongoing periductal inflammation that is well-described in BA. SFTPD is highly expressed in the lung, and it's expression has recently been described on the luminal surface membrane of intrahepatic cholangiocytes of normal and diseased infant cholestatic livers(16). It is plausible for all of the discovered cholangiocyte-predominant IgM autoantibodies that the antibody-antigen complex is associated with complement activation and destruction of cholangiocytes. IgM autoantibodies have been shown to activate and co-localize with C3d in a mouse model of liver ischemia-reperfusion injury(18). Further work on the role of complement activation in BA is warranted.

Limitations within this study include the fact that the autoantigen microarray constitutes linear proteins and therefore antibodies targeting a folded protein configuration may not be detected. There was variability in the types of other liver disease controls and this could theoretically alter the comparisons with BA, as some liver disease controls may have more inflammation than others. With regard to the validation study of the anti-DLL-4 IgG autoantibody, we were limited to patient serum samples between the ages of 12–24 months. Up until 18 months of age the majority of the serum IgG is maternal in origin and therefore our results to detect patient-specific antibodies were not robust. Future studies will be necessary to analyze IgG responses to all 3 of the candidate autoantigens that were associated with IgM autoantibody responses.

Autoantibodies can be generated in response to either intracellular antigens that are released in the setting of excessive cell death, modification of self-antigens during inflammatory responses or molecular mimicry between infectious agents and self-antigens(28). IgM autoantibodies can either be regulatory/ anti-inflammatory (termed “natural autoantibodies”) (9) or actively participate in cellular injury through complement activation, as seen in

models of systemic lupus erythematosus(29), liver ischemia-reperfusion injury(18) and spinal cord injury(17). In the current study, the BA subjects who were positive for all 3 autoantibodies had higher levels of portal tract C3d and desmin (fibrosis marker) staining and had the worst outcome, based on 82% requiring liver transplant in the first 2 years of life. This suggests that the IgM autoantibodies are likely pathogenic, activating complement and contributing to fibrosis. The discovery of autoantibody-mediated complement activation and autoreactive T cells specific to cholangiocyte proteins in BA provides potential targets for therapeutic interventions in the future.

Supplementary Material

Refer to Web version on PubMed Central for supplementary material.

Acknowledgments

Financial Support.

NIH NIDDK R01 DK094937-01A1 (Mack CL)

2T32 DK067009-14 (Brigham D)

U01 Childhood Liver Disease Research Network, NIDDK (DK062497, DK062470, DK062481, DK062456, DK062466, DK062453, DK084538, DK062436, DK062500, DK084536, DK084575, DK103040, DK103149).

The Judith Sondheimer Pediatric GI Fellow Research Fund (Brigham D)

Hewitt/ Andrews Chair in Pediatric Liver Disease Research Fund (Mack CL)

List of Abbreviations.

BA	biliary atresia
ChiLDReN	Childhood Liver Disease Research Network
CHI3L1	chitinase 3-like 1
DLL-4	delta-like ligand 4
SFTPD	surfactant protein D

References.

1. Sundaram SS, Mack CL, Feldman AG, Sokol RJ. Biliary atresia: Indications and timing of liver transplantation and optimization of pretransplant care. *Liver Transpl* 2017;23:96–109. [PubMed: 27650268]
2. Bezerra JA, Wells RG, Mack CL, Karpen SJ, Hoofnagle JH, Doo E, Sokol RJ. BILIARY ATRESIA: Clinical and Research Challenges for the 21(st) Century. *Hepatology* 2018.
3. Kilgore A, Mack CL. Update on investigations pertaining to the pathogenesis of biliary atresia. *Pediatr Surg Int* 2017;33:1233–1241. [PubMed: 29063959]
4. Feldman AG, Tucker RM, Fenner EK, Pelanda R, Mack CL. B cell deficient mice are protected from biliary obstruction in the rotavirus-induced mouse model of biliary atresia. *PLoS One* 2013;8:e73644.

5. Bednarek J, Traxinger B, Brigham D, Roach J, Orlicky D, Wang D, Pelanda R, et al. Cytokine-Producing B Cells Promote Immune-Mediated Bile Duct Injury in Murine Biliary Atresia. *Hepatology* 2018;68:1890–1904. [PubMed: 29679373]
6. Bove KE, Sheridan R, Fei L, Anders R, Chung CT, Cummings OW, Finegold MJ, et al. Hepatic Hilar Lymph Node Reactivity at Kasai Portoenterostomy for Biliary Atresia: Correlations With Age, Outcome, and Histology of Proximal Biliary Remnant. *Pediatr Dev Pathol* 2018;21:29–40. [PubMed: 28474973]
7. Press JL. Neonatal immunity and somatic mutation. *Int Rev Immunol* 2000;19:265–287. [PubMed: 10763712]
8. Holladay SD, Smialowicz RJ. Development of the murine and human immune system: differential effects of immunotoxicants depend on time of exposure. *Environ Health Perspect* 2000;108 Suppl 3:463–473.
9. Merbl Y, Zucker-Toledano M, Quintana FJ, Cohen IR. Newborn humans manifest autoantibodies to defined self molecules detected by antigen microarray informatics. *J Clin Invest* 2007;117:712–718. [PubMed: 17332892]
10. Lu BR, Brindley SM, Tucker RM, Lambert CL, Mack CL. alpha-enolase autoantibodies cross-reactive to viral proteins in a mouse model of biliary atresia. *Gastroenterology* 2010;139:1753–1761. [PubMed: 20659472]
11. Pang SY, Dai YM, Zhang RZ, Chen YH, Peng XF, Fu J, Chen ZR, et al. Autoimmune liver disease-related autoantibodies in patients with biliary atresia. *World J Gastroenterol* 2018;24:387–396. [PubMed: 29391761]
12. Ayoglu B, Schwenk JM, Nilsson P. Antigen arrays for profiling autoantibody repertoires. *Bioanalysis* 2016;8:1105–1126. [PubMed: 27097564]
13. Barcenas-Morales G, Jandus P, Doffinger R. Anticytokine autoantibodies in infection and inflammation: an update. *Curr Opin Allergy Clin Immunol* 2016;16:523–529. [PubMed: 27755185]
14. Shen Z, Liu Y, Dewidar B, Hu J, Park O, Feng T, Xu C, et al. Delta-Like Ligand 4 Modulates Liver Damage by Down-Regulating Chemokine Expression. *Am J Pathol* 2016;186:1874–1889. [PubMed: 27171900]
15. Huang H, Wu T, Mao J, Fang Y, Zhang J, Wu L, Zheng S, et al. CHI3L1 Is a Liver-Enriched, Noninvasive Biomarker That Can Be Used to Stage and Diagnose Substantial Hepatic Fibrosis. *OMICS* 2015;19:339–345. [PubMed: 26415140]
16. Saka R, Yanagihara I, Sasaki T, Nose S, Takeuchi M, Nakayama M, Okuyama H. Immunolocalization of surfactant protein D in the liver from infants with cholestatic liver disease. *J Pediatr Surg* 2015;50:297–300. [PubMed: 25638623]
17. Narang A, Qiao F, Atkinson C, Zhu H, Yang X, Kulik L, Holers VM, et al. Natural IgM antibodies that bind neopeptides exposed as a result of spinal cord injury, drive secondary injury by activating complement. *J Neuroinflammation* 2017;14:120. [PubMed: 28629465]
18. Marshall K, Jin J, Atkinson C, Alawieh A, Qiao F, Lei B, Chavin KD, et al. Natural immunoglobulin M initiates an inflammatory response important for both hepatic ischemia reperfusion injury and regeneration in mice. *Hepatology* 2018;67:721–735. [PubMed: 28880403]
19. Laban S, Suwandi JS, van Unen V, Pool J, Wesselius J, Hollt T, Pezzotti N, et al. Heterogeneity of circulating CD8 T-cells specific to islet, neo-antigen and virus in patients with type 1 diabetes mellitus. *PLoS One* 2018;13:e0200818.
20. McLaughlin KA, Gulati K, Richardson CC, Morgan D, Bodansky HJ, Feltbower RG, Christie MR. HLA-DR4-associated T and B cell responses to specific determinants on the IA-2 autoantigen in type 1 diabetes. *J Immunol* 2014;193:4448–4456. [PubMed: 25225671]
21. Vermeulen N, de Beeck KO, Vermeire S, Van Steen K, Michiels G, Ballet V, Rutgeerts P, et al. Identification of a novel autoantigen in inflammatory bowel disease by protein microarray. *Inflamm Bowel Dis* 2011;17:1291–1300. [PubMed: 21560193]
22. Zingaretti C, Arigo M, Cardaci A, Moro M, Crosti M, Sinisi A, Sugliano E, et al. Identification of new autoantigens by protein array indicates a role for IL4 neutralization in autoimmune hepatitis. *Mol Cell Proteomics* 2012;11:1885–1897. [PubMed: 22997428]

23. Mack CL, Falta MT, Sullivan AK, Karrer F, Sokol RJ, Freed BM, Fontenot AP. Oligoclonal expansions of CD4+ and CD8+ T-cells in the target organ of patients with biliary atresia. *Gastroenterology* 2007;133:278–287. [PubMed: 17631149]
24. Hadchouel M, Hugon RN, Odievre M. Immunoglobulin deposits in the biliary remnants of extrahepatic biliary atresia: a study by immunoperoxidase staining in 128 infants. *Histopathology* 1981;5:217–221. [PubMed: 7216182]
25. Mack CL, Tucker RM, Lu BR, Sokol RJ, Fontenot AP, Ueno Y, Gill RG. Cellular and humoral autoimmunity directed at bile duct epithelia in murine biliary atresia. *Hepatology* 2006;44:1231–1239. [PubMed: 17058262]
26. Kumagai E, Mano Y, Yoshio S, Shoji H, Sugiyama M, Korenaga M, Ishida T, et al. Serum YKL-40 as a marker of liver fibrosis in patients with non-alcoholic fatty liver disease. *Sci Rep* 2016;6:35282. [PubMed: 27739482]
27. Yan M, Plowman GD. Delta-like 4/Notch signaling and its therapeutic implications. *Clin Cancer Res* 2007;13:7243–7246. [PubMed: 18094402]
28. Suurmond J, Diamond B. Autoantibodies in systemic autoimmune diseases: specificity and pathogenicity. *J Clin Invest* 2015;125:2194–2202. [PubMed: 25938780]
29. Zhang J, Jacobi AM, Wang T, Berlin R, Volpe BT, Diamond B. Polyreactive autoantibodies in systemic lupus erythematosus have pathogenic potential. *J Autoimmun* 2009;33:270–274. [PubMed: 19398190]

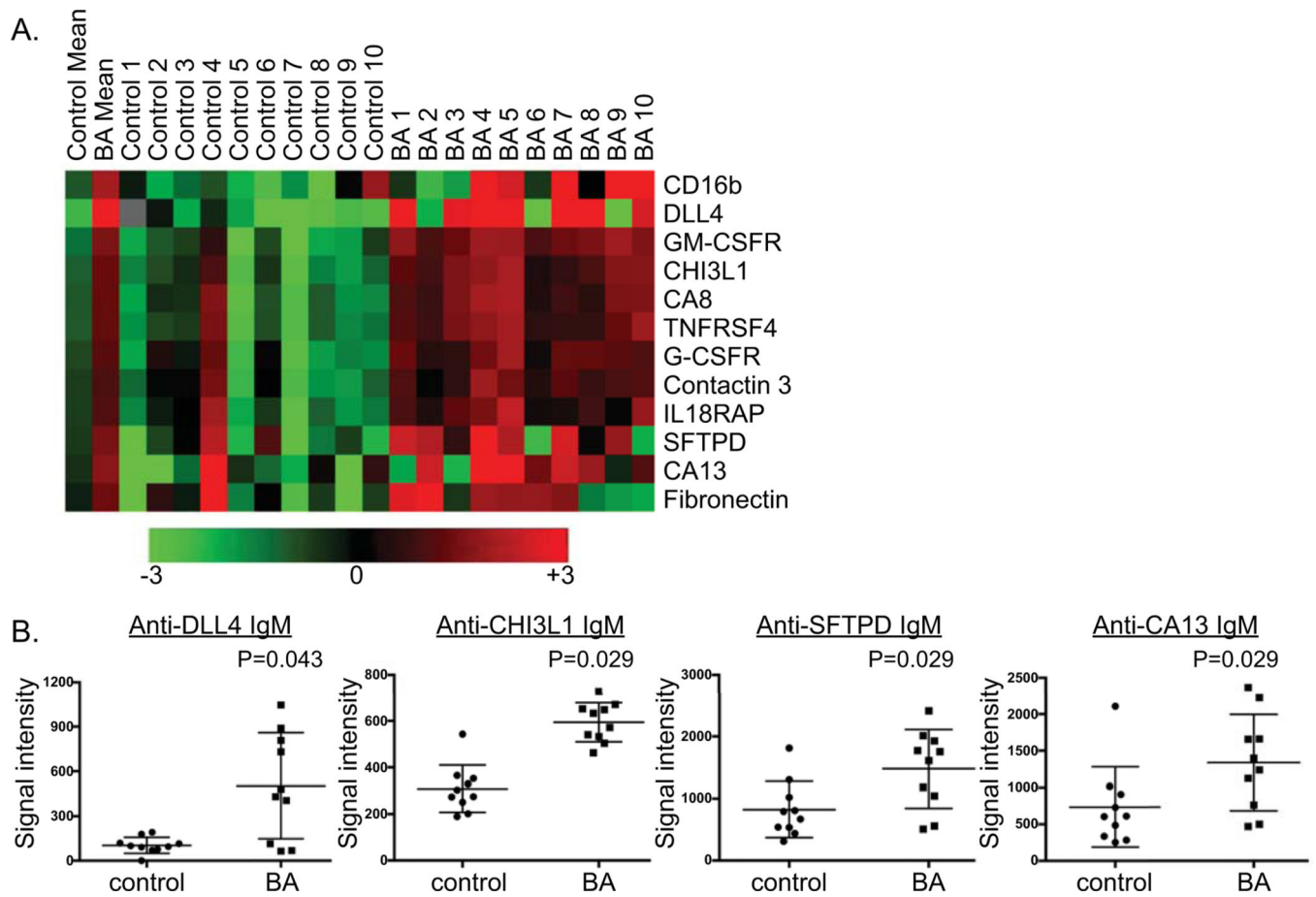


Figure 1. Autoantigen microarray (ProtoArray®) identifies IgM autoantibodies in BA.

A. Heatmap of IgM autoantibodies significantly increased in BA versus other liver disease controls. B. Microarray signal intensity of candidate IgM autoantibodies in BA [candidate autoantibody defined as significantly higher mean value in BA ($P < 0.05$) and at least 50% of BA subjects with autoantibody levels > 1 S.D. above control mean].

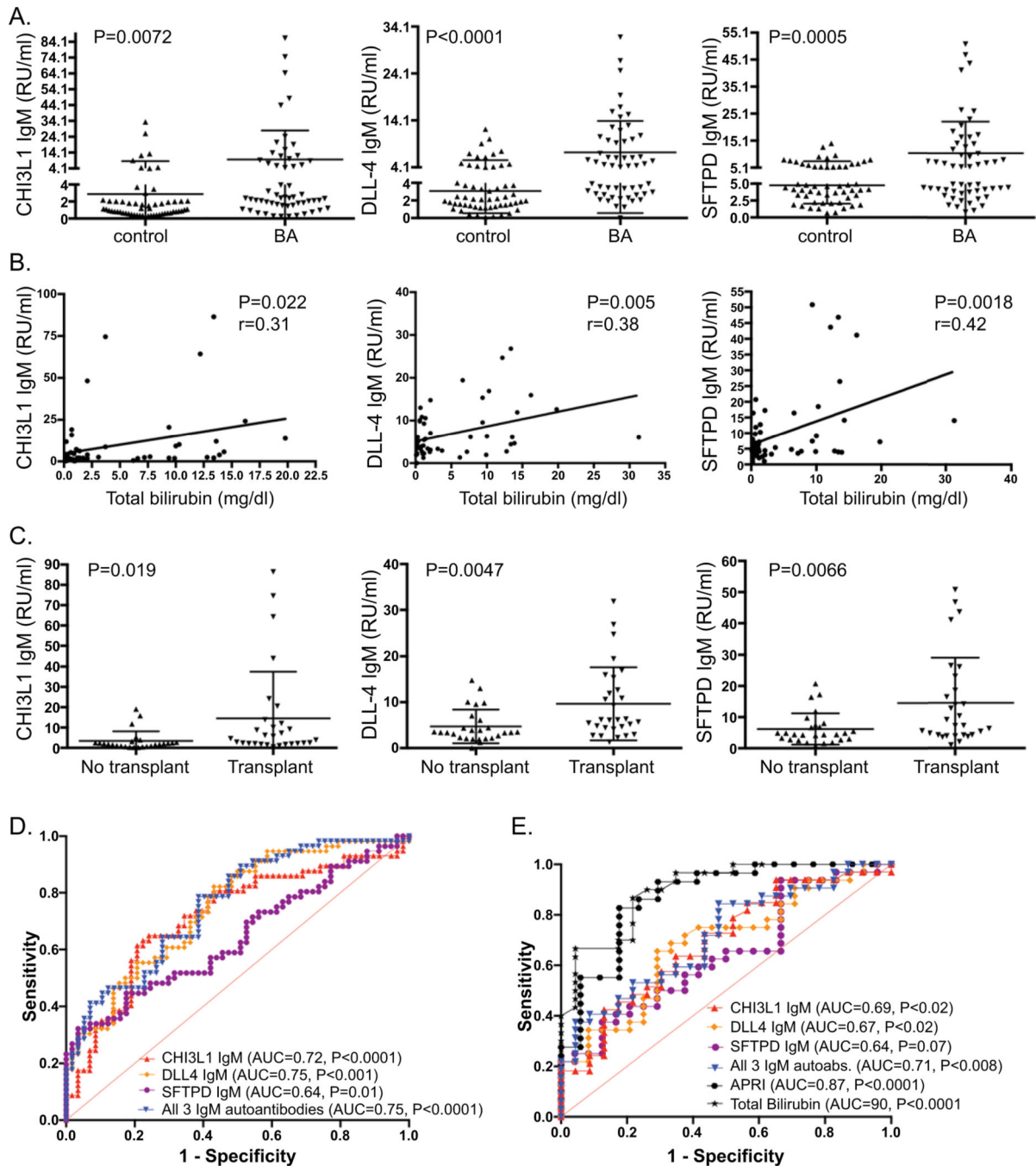


Figure 2. Increased anti-CHI3L1, anti-DLL-4 and anti-SFTPD IgM autoantibodies in BA validation cohort correlates with worse outcomes.

A. Serum levels of IgM autoantibodies in other liver disease controls and BA. B. Spearman correlation of IgM autoantibody level and concurrent serum bilirubin level in BA subjects. C. IgM autoantibody levels at 6–12 months post-Kasai and subsequent need for liver transplant by 2 years of life in BA. D. ROC curves of autoantibodies to predict BA versus non-BA diagnosis. E. ROC curves to predict need for liver transplant in first 2 years of life in BA.

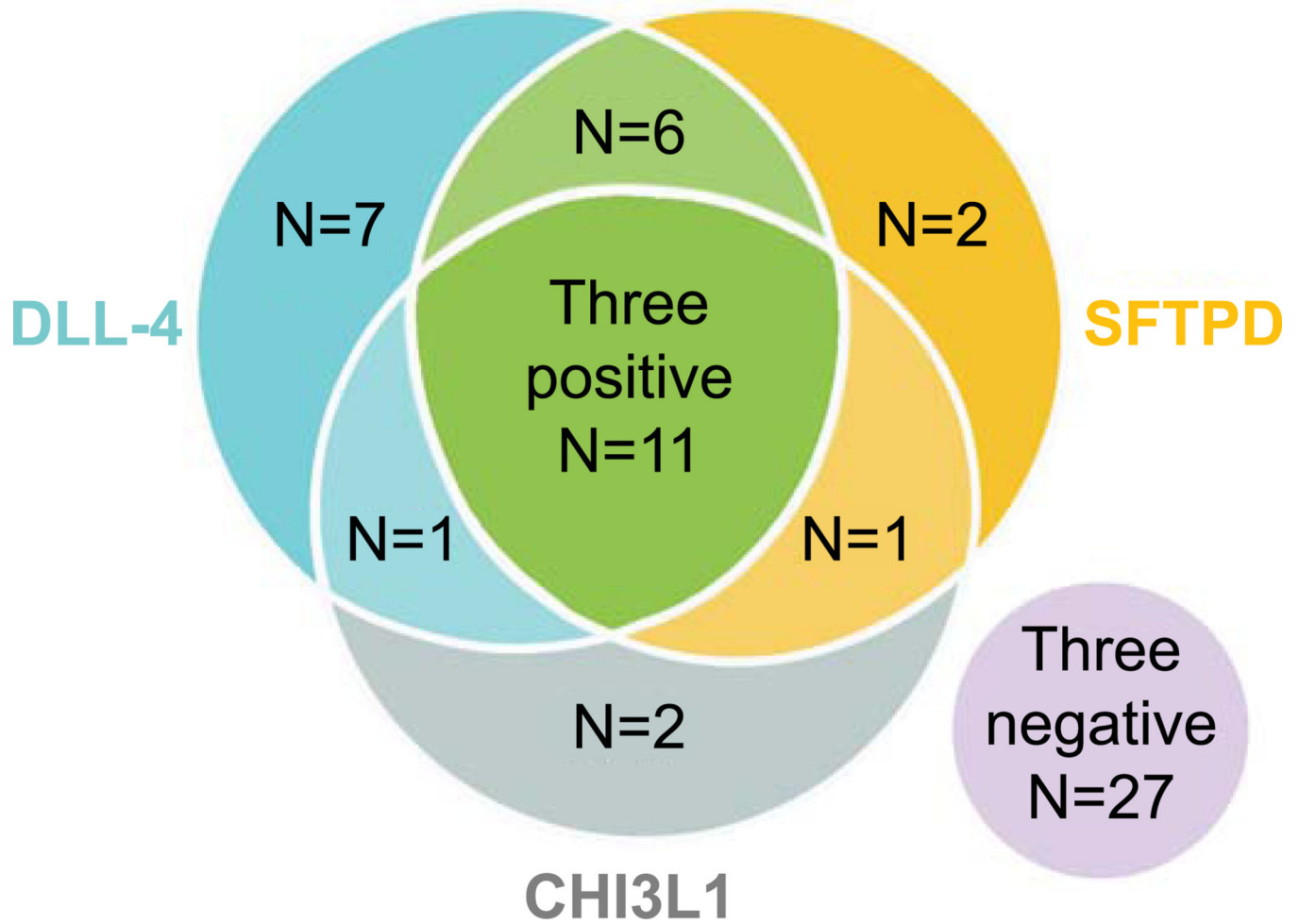


Figure 3. Incidence of IgM autoantibody positivity in BA.

Venn diagram of the number of BA subjects positive for either anti-CHI3L1, anti-DLL-4 and/ or anti-SFTPD IgM autoantibodies.

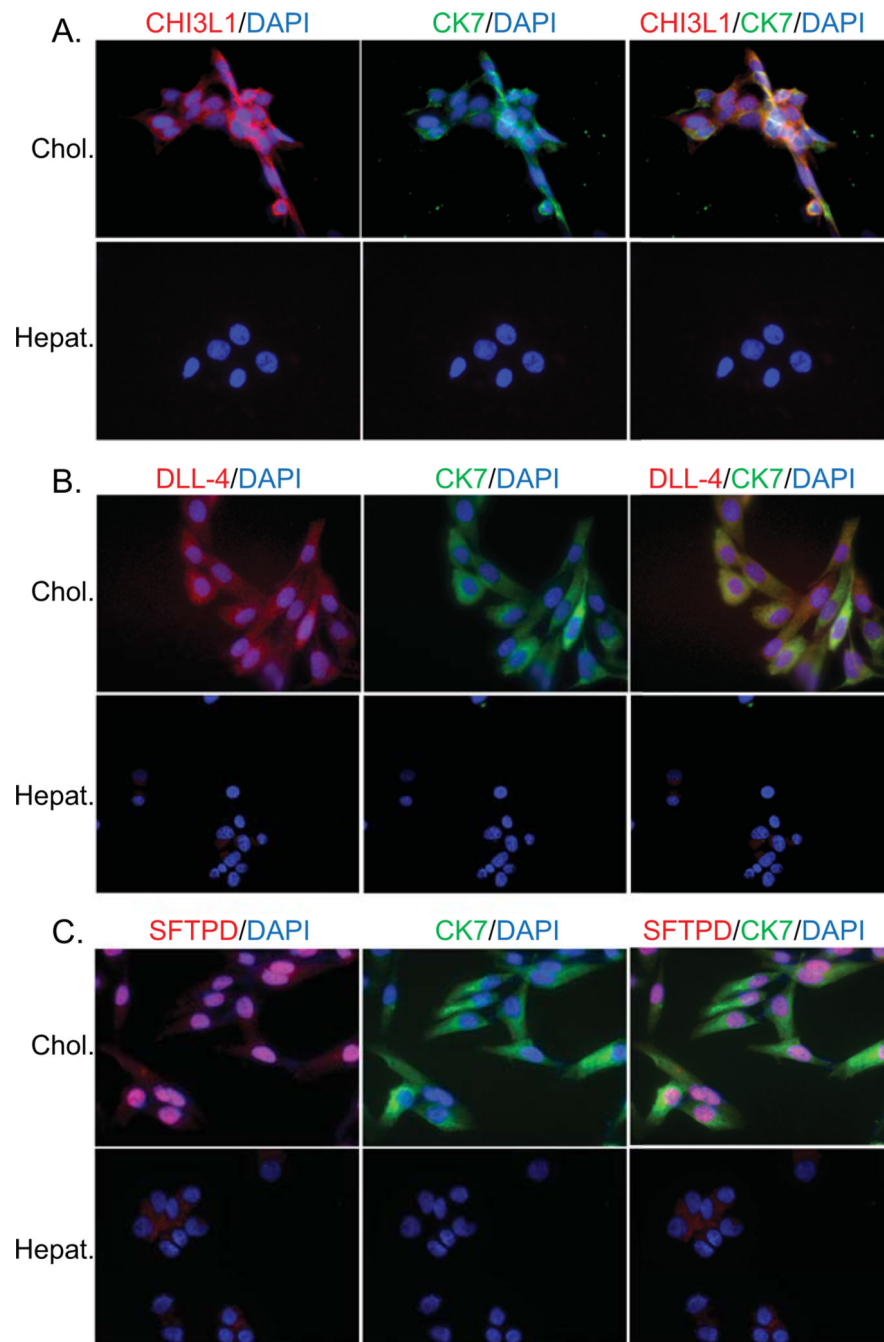


Figure 4. Cholangiocyte-predominant localization of candidate autoantigens.

Immunofluorescence of hepatocyte (Hepat.) or cholangiocyte (Chol.) cell lines with fluorochrome-tagged antibodies to cytokeratin 7 (CK7- cholangiocyte specific; green), CHI3L1 (A.), DLL-4 (B.) or SFTPD (C.) (all autoantigens in red) and counterstained with nuclear DAPI (blue). Co-localization of CK7 and an autoantibody is reflected in yellow color.

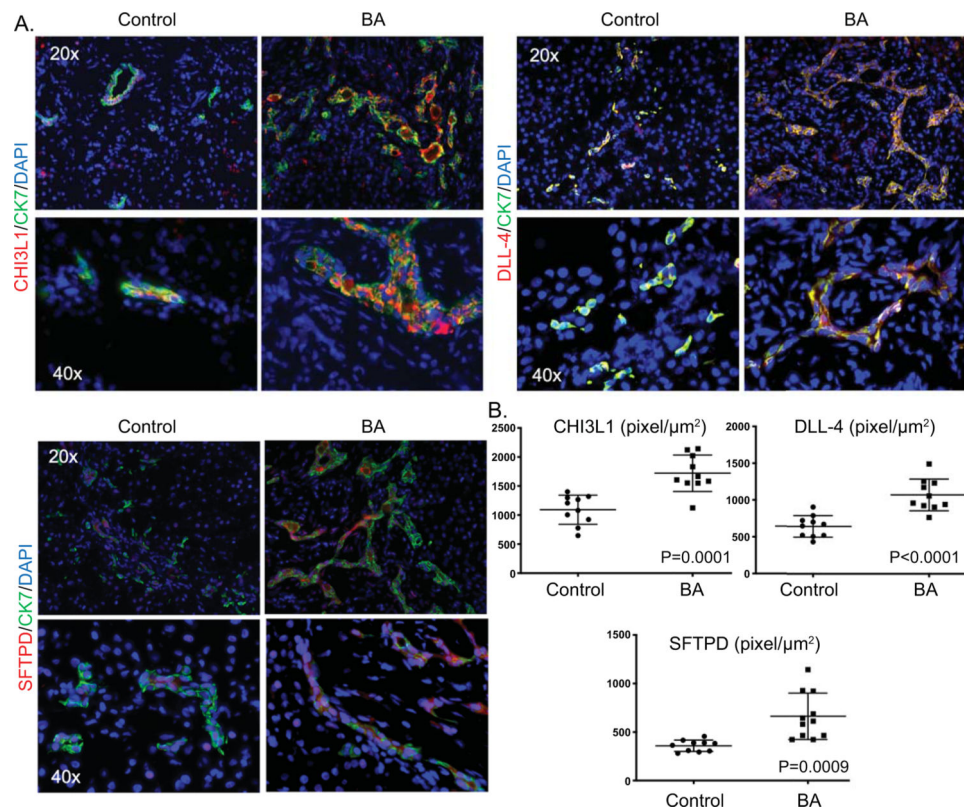


Figure 5. Increased bile duct-predominant candidate autoantigen expression in BA liver tissue. A. Representative immunofluorescence of cytokeratin 7 (CK7; green) and either CHI3L1, DLL-4 or SFTPD (all autoantigens in red), counterstained with nuclear DAPI (blue) on frozen liver tissue from BA patients or controls at time of liver transplant. Co-staining of CK7 and an autoantigen is represented by yellow color. B. Quantitative fluorescence intensity analysis of the amount of autoantigen expression per μm^2 of CK7 positive cells.

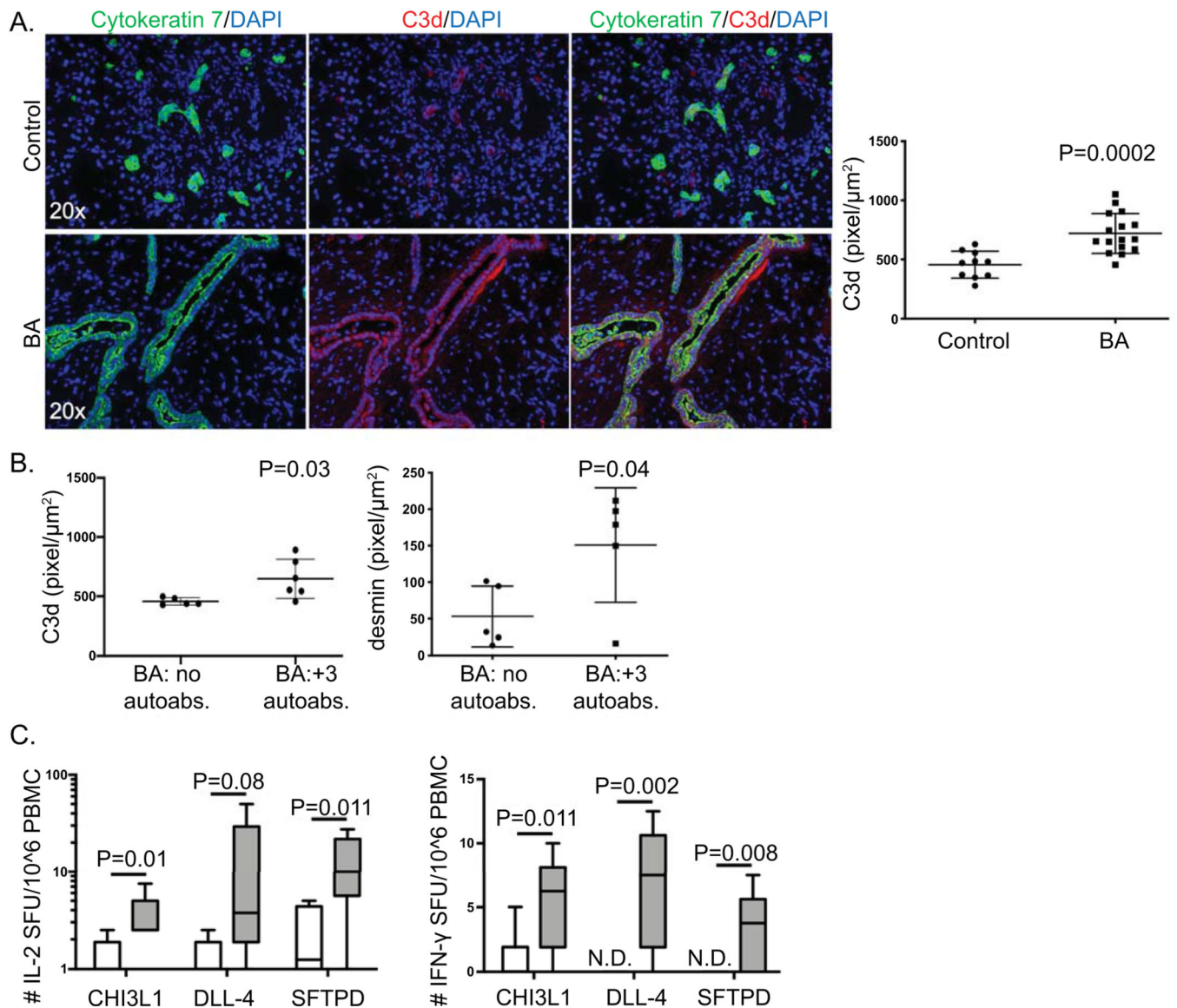


Figure 6. Immune pathways associated with humoral immunity in BA.

(A) Representative immunofluorescence of cytokeratin 7 (green) and C3d (red), counterstained with nuclear DAPI (blue) on frozen liver tissue from controls or BA at time of liver transplant. Right panel: Quantitative fluorescence intensity analysis of C3d expression per μm^2 of cytokeratin 7 positive cells. (B) Quantitative fluorescence intensity analysis of C3d and desmin expression per μm^2 portal tract regions in BA subjects negative for all 3 IgM autoantibodies (BA: no autoabs.) or positive for all 3 IgM autoantibodies (BA: +3 autoabs.) (C) Peripheral blood autoreactive T cells specific to CHI3L1, DLL-4 and SFTPD in BA. Peripheral blood mononuclear cells (PBMCs) were cultured with either CHI3L1, DLL-4, or SFTPD. Autoantigen stimulation of T cells was quantified based on production of IL-2 (a) and IFN- γ (b) by ELISPOT analysis [readout is number of spot forming units (SFU) per million PBMCs]. N.D.- not detected. Positive control PHA- too numerous to count SFU; negative control media alone- N.D..

Table 1.

Validation cohort: demographic information

Descriptor	Controls (N=58)	BA (N=57)	P-value
Age (months)	7.81±1.72	7.95±1.6	0.083 [#]
% female	36	56	0.032 [*]
Ethnicity			
% Caucasian	69	45	0.011 [*]
% African American	9	14	
% Multiracial	9	19	
% Asian	5	12	
% Other	8	7	
Total bilirubin (mean±SD; mg/dL)	3.04±5.57	5.51±6.49	0.017 [#]

* chi-square analysis;

[#] student t-test unpaired samples

Table 2.

BA demographics based on number of positive IgM autoantibodies

Descriptor	Three negative autoantibodies (N=27)	Three positive autoantibodies (N=11)	P-value
Age at serum collection (months)	8.19 ±1.69	7.18 ±1.16	0.08 [#]
Age at time of Kasai (months)	1.64±0.91	2.33±1.94	0.16 [#]
% female	48	73	0.17 [*]
% transplanted by 2 yrs. age	37	82	0.012 [*]
Total bilirubin (mg/dl)	3.13 ±4.47	9.16 ±5.27	0.002 [#]

* chi-square analysis;

[#] student t-test unpaired samples

Author Manuscript

Author Manuscript

Author Manuscript

Author Manuscript